

Normal State Ettingshausen Effect in $\text{La}_{2-x}\text{Sr}_x\text{CuO}_4$

T.Plackowski and M.Matusiak

Institute of Low Temperature and Structure Research,

Polish Academy of Sciences,

50-950 Wrocław, P.O.Box 1410

POLAND

(Submitted to Superconductor Science and Technology, April 2, 1999)

Typeset using REVTeX

Abstract

A method for measurements of small (metallic) Ettingshausen coefficient (P) was developed. The influence of the dominating thermal effects, the Joule and Thomson heats, was eliminated making use of the odd symmetry of the Ettingshausen temperature gradient in respect with reversing of the direction of the magnetic field and electrical current. The method was applied to $\text{La}_{2-x}\text{Sr}_x\text{CuO}_4$ ($x = 0.03 \div 0.35$) high- T_c superconductor in normal state. We have found that in the whole composition range the Ettingshausen coefficient is of the order of $10^{-7} \text{ m}^3\text{K/J}$ which is characteristic of typical metals. The coefficient changes sign from positive to negative near $x \approx 0.07$. Weak variation of P is in contrast to the behavior of other transport coefficients for $\text{La}_{2-x}\text{Sr}_x\text{CuO}_4$, as the thermoelectric power or the Hall coefficient, which have been reported in literature to change their values by more than two orders of magnitude with Sr doping.

I. INTRODUCTION

Since the discovery of high- T_c (HTC) superconductors their normal state properties are a subject of extensive investigations. Many of them, as the electrical resistivity ρ , the Hall effect R_H or the thermoelectric power S , exhibit some universal behavior in function of charge carrier doping. The universal behavior of the latter quantity is well known, for many of the HTC families the thermopower changes sign at optimal carrier concentration [1]. The linearity of resistivity for the optimally doped samples in wide temperature region is also one of their most well known features [2]. The Hall coefficient for optimally doped samples varies as $1/T$, which results in the $1/T^2$ dependence of the Hall mobility, μ_H . Then it appeared that the $1/T^2$ dependence of μ_H is more universal. It applies not only to the optimally doped, but also to the under- and overdoped materials [3].

In this work we present the measurements of the Ettingshausen coefficient, one of the less known transport coefficients. Our aim was to complement the present knowledge of the normal state properties of HTC materials, and, hopefully, to search for some new universalities. The Ettingshausen effect is a thermal analog of the Hall effect (the definition and sign convention are shown in Fig. 1). The difference with respect to the Hall effect lies in the fact that the temperature difference is measured in the direction perpendicular to both the current and field directions, instead of the voltage difference.

The Hall and Ettingshausen effects are two of the four transversal magneto-thermal effects:

$$\begin{aligned}\nabla\Phi_{\perp} &= R_H \vec{j} \times \vec{B}, \text{ the Hall effect,} \\ \nabla T_{\perp} &= P \vec{j} \times \vec{B}, \text{ the Ettingshausen effect,} \\ \nabla\Phi_{\perp} &= Q \nabla T \times \vec{B}, \text{ the Nernst effect,} \\ \nabla T_{\perp} &= S_{RL} \nabla T \times \vec{B}, \text{ the Righi-Leduc effect,}\end{aligned}$$

where R_H , P , Q , S_{RL} are the respective coefficients, $\nabla\Phi_{\perp}$ and ∇T_{\perp} are the transversal gradients of electrical potential and temperature, respectively, caused by the presence of

magnetic field (\vec{B}) perpendicular to the electrical current (\vec{j}) or heat flux ($\vec{q} \sim \nabla T$). All these coefficients are interconnected by three fundamental relations which were considered by P.W.Bridgman [4] in terms of thermodynamics of reversible processes:

$$\begin{aligned} Q &= \frac{\kappa}{T} P, \\ Q &= \frac{\mu_T}{\rho} R_H, \\ P &= \frac{\mu_T T}{\kappa} S_{RL}, \end{aligned}$$

where κ is the total thermal conductivity and μ_T is the Thomson coefficient .

The theory of the Ettingshausen effect for semiconductors was considered in [5], and for metals in [6]. Only few measurements of the Ettingshausen effect in different materials were carried out up to date. Typical measured values of the Ettingshausen coefficients for semiconductors are positive and of the order of $10^{-2} \div 10^{-4}$ m³K/J (Ge: [7]; Si: [8]; PbSe, PbTe: [9]). Typical values of the Ettingshausen coefficient for metals are much lower then for semiconductors and are of the order $10^{-7} \div 10^{-8}$ m³K/J. A negative Ettingshausen coefficient was observed for Ag, Cd, Cu, Fe, Zn and Au, whereas positive for Al, Co and Ni. The Ettingshausen effect and the Hall effect have opposite signs for Al, Cd, Fe, Ni and Zn, whereas the same signs for Ag, Co, Cu and Au [10,4]. The Ettingshausen coefficient is much higher for semi-metals ($\sim 10^{-4}$ m³K/J for Sb and $\sim 10^{-3}$ m³K/J for Bi [4]) and for rare earths ($\sim 10^{-3}$ m³K/J for Y, Gd, Tb and Dy [11]).

According to our knowledge, no measurements of the Ettingshausen effect were carried out in HTC superconductors in normal state. Few works were devoted to the normal state Nernst effect: for Tl-2212 [12], YCBO [13] and NdCeCuO [14].

In the present work we have chosen the La_{2-x}Sr_xCuO₄ (LSCO) solid solution ($x = 0.03 \div 0.35$). This compound exhibits full range of behaviors versus chemical composition, which is characteristic of the layered copper-oxide superconductors. The carrier concentration may be controlled by the Sr concentration x . One could therefore investigate the doping dependence from the semiconducting region ($x \lesssim 0.05$), through the underdoped ($0.05 \lesssim x \lesssim 0.17$) and overdoped ($0.17 \lesssim x \lesssim 0.30$) superconducting regions, up to the heavily doped metallic region with no superconductivity ($x \gtrsim 0.30$) [15]. Moreover, LSCO has a simple crystal structure with single CuO₂ layers. It has neither Cu-O chains as in YBa₂Cu₃O_{7- δ} nor complicated modulation of the separating and spacing layers as in Bi- and Tl-based materials. All our samples have been characterized by X-ray and electrical resistivity measurements.

II. EXPERIMENTAL

A. Samples

Polycrystalline samples of La_{2-x}Sr_xCuO₄ were produced following the standard solid state technique from high purity La₂O₃, SrCO₃ and CuO substrates. The powders were mixed and prefired in air at 950 °C for 24 h. After pulverization, the materials were mixed, pressed and sintered at 1000 °C for 60 h. Then they were reground, pelletized and, except one sample, refired at 1050 °C for 72 h in oxygen under pressure of 1 bar. Only the sample

of $\text{La}_{1.65}\text{Sr}_{0.35}\text{CuO}_4$ was sintered in oxygen under the pressure of 300 bar at 1000 °C for 48 h. All products were confirmed to be single phase by powder X-ray diffraction. The values of the critical temperature measured by the electrical resistivity measurements are shown in Table 1.

Table 1. Critical temperatures of the $\text{La}_{2-x}\text{Sr}_x\text{CuO}_4$ samples.

x (Sr)	0.03	0.05	0.10	0.15	0.20	0.25	0.30	0.35
T_c [K]	0	0	28.6	36.0	30.2	18.0	10.2	0

B. Choice of the experimental configuration

The Ettingshausen effect is usually very small, hence it might be easily overridden by other thermal effects, as the Joule and Thomson effects. Especially, the Joule heat may particularly hinder the detection of the Ettingshausen effect. When measuring this effect a strong electrical current should be passed through the sample thus evolving a large amount of energy at the electrical contacts, which electrical resistance is usually much higher than that of the sample. Therefore, some places of the sample should be thermally anchored to a large mass of constant temperature to carry the Joule heat away. On the other hand, the sample should be located in adiabatic conditions since the thermal gradient is the quantity to be measured. For the above reason we started from computer modelling of different possible experimental setups, with different patterns of sample anchoring (e.g. on corners, along the longest side, etc.). In all cases we have supposed that the sample should have a shape of a flat slab with the shortest dimension parallel to the magnetic field, since the temperature difference due to the Ettingshausen effect is inversely proportional to that dimension (in analogy to the Hall effect). The configuration we have finally chosen is presented Fig. 2.

The ends of the sample (A) were attached to two copper bars (B) using the Au:In alloy and silver paint, making both good electrical and thermal contacts. The typical contact resistance amounted to $0.5 \div 2 \Omega$ and was much higher than the sample resistance. The bars (B) were electrically insulated from the copper support (C), but their good thermal connection to the support was ensured by a relatively large area of the contacts. The sample was also surrounded by a thick copper screen (D) screwed on the support (C). The carbon-glass thermometer (E) was located within support (C). The whole assembly was placed in a gas-flow cryostat. A differential copper-constantan-copper thermocouple was attached to the sides of the sample. This type of thermocouple has relatively large sensitivity at room temperature ($\alpha = 40.5 \mu\text{V/K}$). Moreover, since only the middle segment was made of constantan, the total resistivity of the thermocouple amounted to few ohms only, reasonable reducing the thermal voltage noise. Next advantage was that only copper leads were connecting the thermocouple junctions on the sample with the Keithley 182 nanovoltmeter input, thus avoiding all detrimental EMF's (the only lead solderings were thermally anchored to the support C). No detectable influence of the magnetic field on the thermocouple voltage have been found.

Providing that the length of the sample is much greater than its width, in our configuration the Ettingshausen coefficient P may be calculated directly from the definition:

$$\Delta T_{\text{Ett}} = P J_x B_z / d$$

where ΔT_{Ett} is the temperature difference between both sides of the sample due to the Ettingshausen effect, J_x is the electrical current, B_z is the magnetic induction and d is the sample thickness. All our samples had thickness of 0.25-0.35 mm, width of 2.5-3 mm and length of 9-10 mm.

C. Influence of the Joule effect

The temperature distribution on the sample surface due the Ettingshausen effect was presented in Fig. 3a. Our calculations have shown that in the centre of the sample this distribution is independent on the temperature distribution caused by the Joule effect, which is shown in Fig. 3b. In other words, the difference ΔT_{Ett} remains unaffected by the Joule heat, even if the values of the temperature gradient along the sample are much higher then the transversal gradient. The reason is that the gradients produced by the two effects are perpendicular. However, an inevitable mismatching of the thermocouple junctions positions causes that the Joule effect also may significantly contribute to the total temperature difference measured:

$$\Delta T = T_2 - T_1 = \pm \Delta T_{Ett} + \Delta T_{Joule}$$

Depending on particular mounting, the ΔT_{Joule} difference may be of any sign. Its value, which is approximately proportional to J^2 , may be much higher then ΔT_{Ett} . Fortunately, the ΔT_{Ett} difference changes its sign upon reversing the direction of both electrical current and magnetic field, whereas ΔT_{Joule} difference does not. This feature was used to extract the Ettingshausen effect from the background.

D. Influence of the Thomson effect

There is another effect interfering with determination of the Ettingshausen temperature difference ΔT_{Ett} - namely the Thomson effect. Because of our experimental arrangement a temperature gradient along the sample is present (see Fig. 3a), so the total heat q produced per time unit in the sample (without magnetic field) consists of two components:

$$\dot{q}(x) = J_x^2 \rho - \mu_T J_x \frac{dT(x)}{dx}$$

The first term is the Joule heat, the second - the Thomson heat; ρ denotes the electrical resistivity and μ_T - the Thomson coefficient. According to our knowledge, the values of the Thomson coefficient for HTC materials are unknown. However, they should be of the order of the Seebeck coefficient, because of the Kelvin relation, $\mu_T = T dS/dT$. The Thomson effect causes that the temperature distribution along the sample slightly changes upon changing the direction of the electrical current - see Fig. 4. Thus, the total temperature difference measured crosswise the sample should be expressed as:

$$\Delta T = T_2 - T_1 = \pm \Delta T_{Ett} + \Delta T_{Joule} \pm \Delta T_{Thomson}$$

The $\Delta T_{Thomson}$ difference changes sign upon changing the direction of the electrical current, but, fortunately, it is insensitive to the magnetic field. Hence, the measurements of ΔT in function of magnetic field still give a chance to extract the effect of interest, ΔT_{Ett} .

In the course of our experiments we have sometimes observed that during prolonged measurements on the same sample the values of the ΔT_{Joule} and $\Delta T_{Thomson}$ changed significantly (including the sign change for $\Delta T_{Thomson}$), whereas the ΔT_{Ett} remained unaffected. This observation is not surprising since ΔT_{Joule} and $\Delta T_{Thomson}$ are just a result of the mismatching of the thermocouple junctions which can be effectively changed by thermocycling.

E. Influence of the electrical contacts heating and of the gas cooling

The resistance of the sample contacts was usually approximately one order of magnitude higher than that of sample itself, so most of the electrical energy was released within the contacts. The only consequence for the temperature distribution within the sample is that the curves shown in Fig.4 are shifted upwards, with no change of both the longitudinal and transversal temperature gradients. However, due to relatively large electrical current values we were using (up to 0.5 A) the sample would be heated up by several kelvins in respect of its surrounding (i.e. the support C with thermometer and the screen D, see Fig. 2). Therefore, in order to keep the temperature of the sample possibly close to that of thermometer we decided to perform all measurements in helium gas atmosphere under ambient pressure, despite that it will influence all temperature gradients in the sample and its support. We can assume that the gas has the temperature of the support. Thus, the gas is colder than the sample heated by the electrical contacts. Therefore, one could expect that the longitudinal temperature distributions presented in Figures 3a and 4 would be substantially flatten, or even inverted, depending on the ratio of the Joule heating to the gas cooling efficiency. The diminishing of the transversal gradient due to the Ettingshausen effect depends only on the gas cooling efficiency. Therefore, it is possible to set the experimental conditions so that the gas cooling is weak enough to do not disturb the Ettingshausen effect significantly, but to reduce substantially the detrimental longitudinal gradients. Indeed, in tests, in which one of the thermocouple junctions was moved onto the bar B, we have observed that for low values of the measurement current the middle of the sample may be colder than its ends (see Fig. 5). Moreover, reducing high temperature gradients by gas cooling should also result in diminishing the influence of non-linear energy exchange by radiation.

To check the influence of the gas cooling on the results we have performed several measurements changing pressure of helium gas in the range of 30÷1030 mbar. It has been observed that the value of the measured Ettingshausen coefficient is insensitive to the pressure within the measurement error. In contrast, the reduction of the pressure from 1030 mbar to 30 mbar resulted in increase of the ΔT_{Joule} difference by approximately 3 times. The $\Delta T_{Thomson}$ difference was also found to be quite sensitive to the pressure, even that sign changes were observed.

F. Measurements strategy

A typical measurements sequence without magnetic field is presented in Fig. 6. For each electrical current value several readings of the thermocouple voltage were taken, with alternatively changing the current direction. A delay of 60-120 seconds was applied after each current reversal to allow the steady-state to build up. The average value of the measured voltage for a given current value (ΔT_{Joule}) was increasing approximately proportionally to J^2 , as it might be expected for the Joule effect (see the upper insert). Changing the current direction resulted in a smaller voltage variations, which amplitude was found to be dependent on the electrical current value (see the lower insert). We suppose that the Thomson effect is responsible for these variations. In this paper we will call this amplitude $\Delta U_{\pm J}$ (an amplitude of the thermocouple voltage variations due to reversing of the electrical current). The Thomson temperature difference may be calculated from the equation:

$$\Delta U_{\pm J} = \alpha(\Delta T_{Thomson})$$

where α is the thermocouple sensitivity. As expected from our computer simulations, we have not observed any universal dependence of $\Delta U_{\pm J}$ on electrical current. For some cases $\Delta U_{\pm J}$ changed its sign for a certain value of the current (with no magnetic field).

Application of the magnetic field causes the Ettingshausen effect and now the amplitude $\Delta U_{\pm J}$ is a sum of two contributions:

$$\Delta U_{\pm J} = \alpha(\Delta T_{Thomson} + \Delta T_{Ett})$$

A typical measurement sequence in magnetic field and with constant electrical current is shown in Fig. 7. The influence of the Ettingshausen effect is clearly visible. The measured amplitude $\Delta U_{\pm J}$ strongly depends on the field strength. The insert demonstrates the values of $(\Delta T_{Thomson} + \Delta T_{Ett}) = \Delta U_{\pm J}/\alpha$ for different values of magnetic field fitted by a linear function. The Ettingshausen coefficient is calculated from the slope A of this line using the formula:

$$P = A \frac{d}{J}$$

The linearity of the dependence of the Ettingshausen effect on electrical current value may be checked by plotting the differences $\Delta U_{\pm J}(B) - \Delta U_{\pm J}(B = 0)$ versus current (see Fig. 8).

Taking into account all the above considerations we have developed a measurements strategy which is illustrated in the Fig. 9. For a particular sample we started from measuring of the current dependencies of the $\Delta U_{\pm J}$ amplitude at $B = +8, 0$ and -8 T. Hence, we were able to check the linearity of $\Delta U_{\pm J}$ with the electrical current value. Then, we chose a value of current for measuring the field dependency of $\Delta U_{\pm J}$ amplitude. If possible, we chose a value of J for which $\Delta U_{\pm J}(B = 0)$ was close to zero, in order to avoid the influence of another interfering effect connected with the Righi-Leduc phenomenon, which is defined as:

$$\nabla T_{RL} = S_{RL} B_z \nabla T_x$$

where S_{RL} is the Righi-Leduc coefficient. This effect may result in another contribution to the transverse thermal gradient if a longitudinal thermal gradient is present. Fortunately, the lack of the Thomson effect is an indication of small longitudinal gradients and in this case the Righi-Leduc effect may be neglected. Moreover, to reduce additionally the influence of the Joule and Thomson effects all measurements were performed at ~ 1 bar of helium gas.

III. RESULTS AND DISCUSSION

The method described in this paper allows measurements of Ettingshausen effect of typical for metals, small value. The effect consists in the transversal thermal gradient appearing due to the electrical current flow in the presence of the perpendicular magnetic field. Since this weak thermal effect may be easily overridden by the Joule and Thomson effects a special measures have been taken to extract it from the background. The sample ends were thermally anchored to a large mass to carry away the Joule heat. To eliminate the influence of the longitudinal thermal gradients due to the Joule and Thomson effects the odd symmetry of the Ettingshausen temperature difference in respect with the direction of the magnetic field and electrical current have been exploited.

The values of the measured Ettingshausen coefficients for $\text{La}_{2-x}\text{Sr}_x\text{CuO}_4$ are shown in Fig. 10. For each composition 2 or 3 samples were investigated. For each sample several measurement runs were carried out and the results were averaged. All the coefficients are of the order of $10^{-7} \text{ m}^3\text{K/J}$, what is typical value for good metals, in contrast to the semiconductors, where values higher by several orders of magnitude are expected (see the Introduction). The Ettingshausen coefficient for $\text{La}_{2-x}\text{Sr}_x\text{CuO}_4$ changes the sign: it is positive only for low Sr concentration ($x = 0.03$ and 0.05), for all other compositions negative values were observed. This is also in contradistinction to the situation of semiconductors, where only positive values are predicted by the theory [5] and found experimentally (see Introduction). The overall weak compositional dependence is somehow surprising, since the other transport coefficients for $\text{La}_{2-x}\text{Sr}_x\text{CuO}_4$ were found to be strongly dependent on Sr/La substitution. It was shown [16,17] that for the compositional range $x = 0.05 \div 0.35$ the Hall coefficient decreases by more than two orders of magnitude. Similar strong variation with composition was found for thermoelectric power [18,19].

IV. ACKNOWLEDGMENTS

The work was supported by the Polish State Committee for Scientific Research under contract No. 2PO3B 11613.

Figure captions

Figure 1 The sign convention for a positive Ettingshausen effect.

Figure 2 An experimental setup used for measurements of the Ettingshausen effect. See text for details.

Figure 3 The temperature distribution on the sample area due the Ettingshausen effect (a) and the temperature distribution along the sample due to the Joule effect (b). The mismatching of the thermocouple junctions positions was exaggerated to indicate how the Joule effect may contribute to the measured temperature difference $\Delta T = T_2 - T_1$. Calculated by the finite-elements method.

Figure 4 The temperature distribution along the sample due to the Joule and Thomson effects for two directions of the electrical current. The difference between two curves was exaggerated for sake of clarity. Calculated by the finite-elements method.

Figure 5 A realistic temperature distribution along the sample for different values of the measurement current (calculated by the finite-elements method). The Joule and Thompson effects within the sample, the Joule effect in the electrical contacts and the cooling by the surrounding gas have been taken into account. The sample ends are warmer in respect with the support due to the Joule heating of the contacts. It is assumed that the gas has the same temperature as the support. The insert shows the results of the tests, in which one of the thermocouple junctions was moved onto the bar B (see Fig. 2) and the longitudinal gradient $\Delta T_{l/2}$ has been measured.

Figure 6 An exemplary measurement sequence performed on $\text{La}_{1.75}\text{Sr}_{0.25}\text{CuO}_4$ sample at room temperature without magnetic field. The thermocouple voltages are plotted versus the successive reading numbers. The direction of the electrical current was alternatively changed from reading to reading. Our convention is that J is positive for odd reading numbers, which are denoted by filled circles. Even numbers are denoted by empty circles. The upper insert shows the average voltage for each value of the current versus the current, i.e. the result of the Joule effect (the thermocouple sensitivity is denoted by α). The variations of the voltage with the current direction are due to the Thomson effect. The amplitude of these variations $\Delta T_{Thomson} = \Delta U_{\pm J}/2\alpha$ versus current value is shown on the lower insert.

Figure 7 An exemplary measurement sequence performed on $\text{La}_{1.75}\text{Sr}_{0.25}\text{CuO}_4$ sample at room temperature for a constant electrical current and in varied magnetic field (see also the caption of Fig. 6). A plot of the amplitude $(\Delta T_{Thomson} + \Delta T_{Ett}) = \Delta U_{\pm J}/2\alpha$ versus B is shown in the insert.

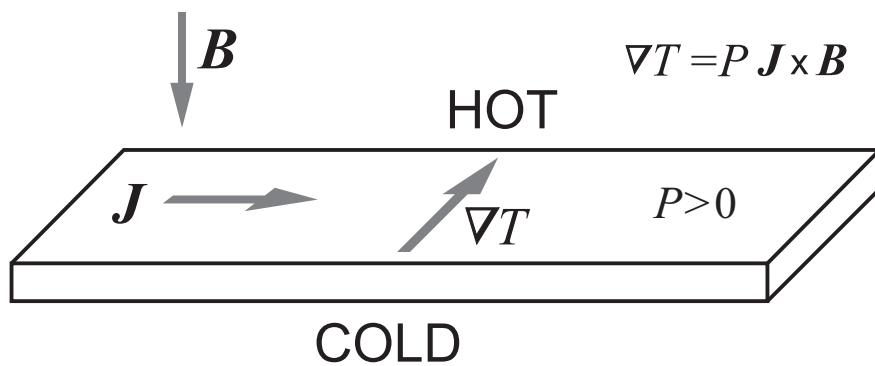
Figure 8 A plot of the amplitude $(\Delta T_{Thomson} + \Delta T_{Ett}) = \Delta U_{\pm J}/2\alpha$ versus electrical current for different values of the magnetic field. The insert shows the differences $(\Delta U_{\pm J}(B) - \Delta U_{\pm J}(B = 0))/2\alpha = \pm \Delta T_{Ett}$ (α is the thermocouple sensitivity).

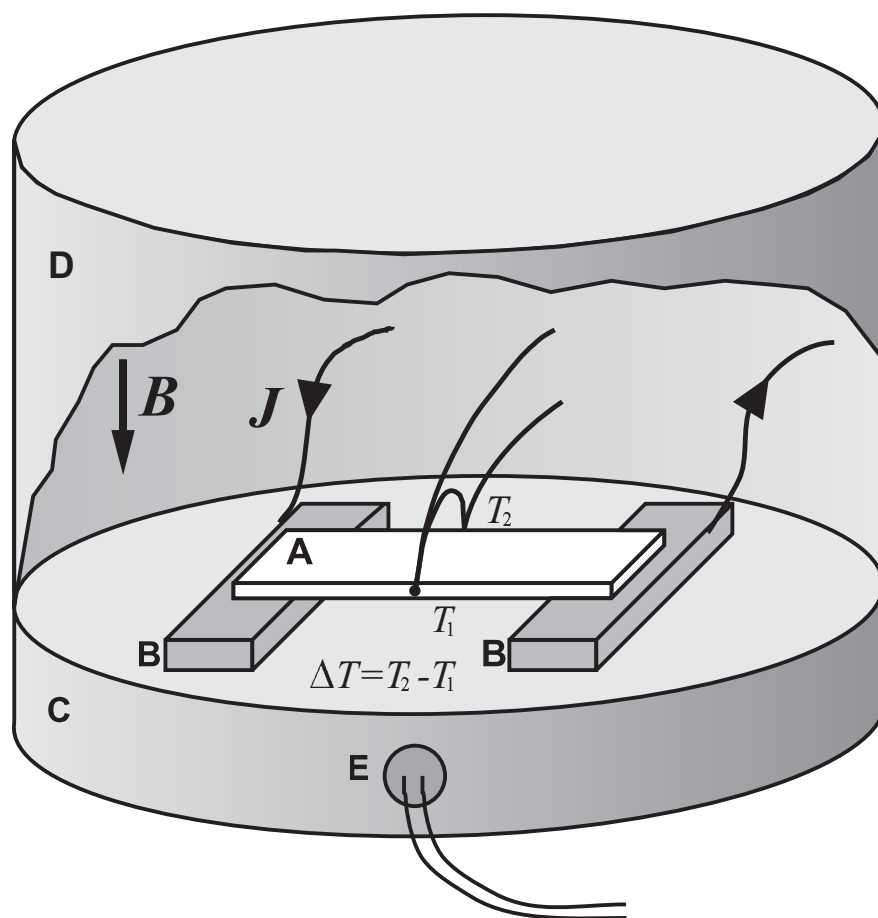
Figure 9 A sketch of the experimental procedure for measurements of the Ettingshausen effect. At each point on the (B, J) plane several readings of the transversal temperature gradient have been taken for both current directions (see Figures 6 and 7).

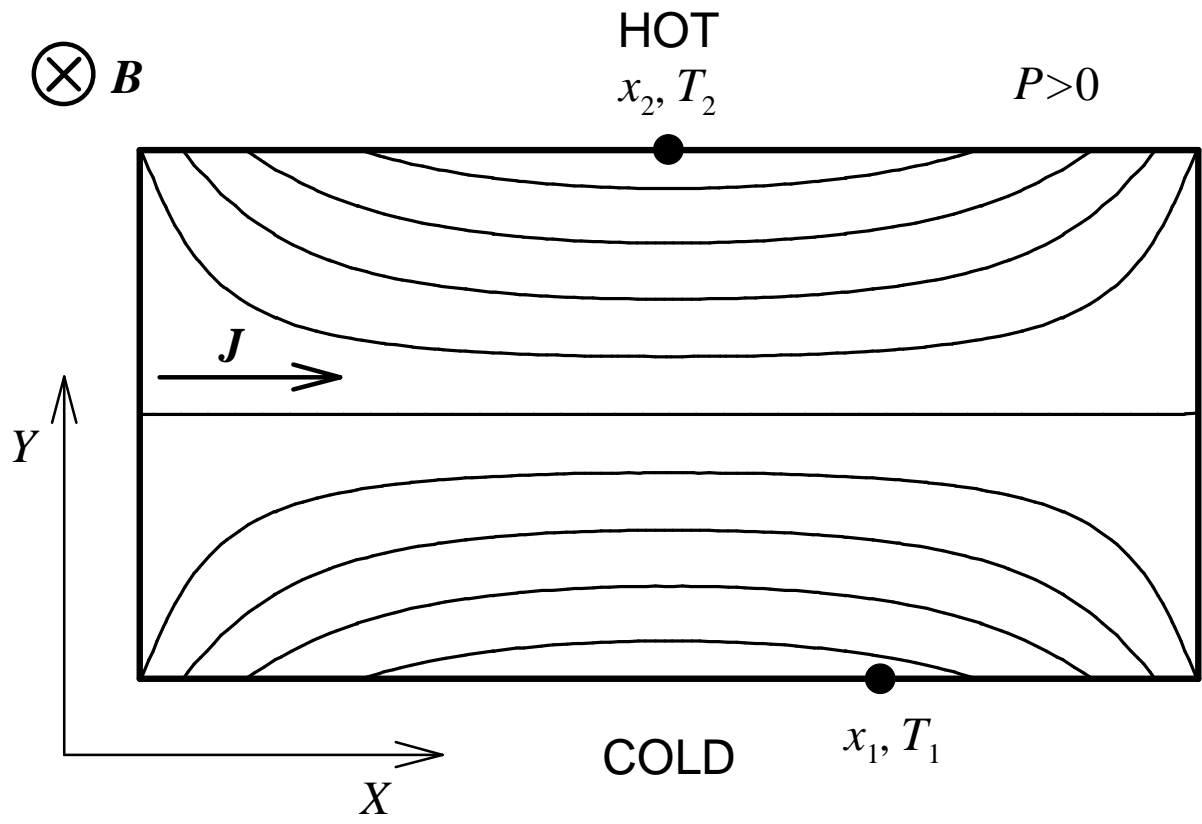
Figure 10 The room temperature Ettingshausen coefficients for $\text{La}_{2-x}\text{Sr}_x\text{CuO}_4$. The error bars denote the scatter of experimental values obtained for a particular composition.

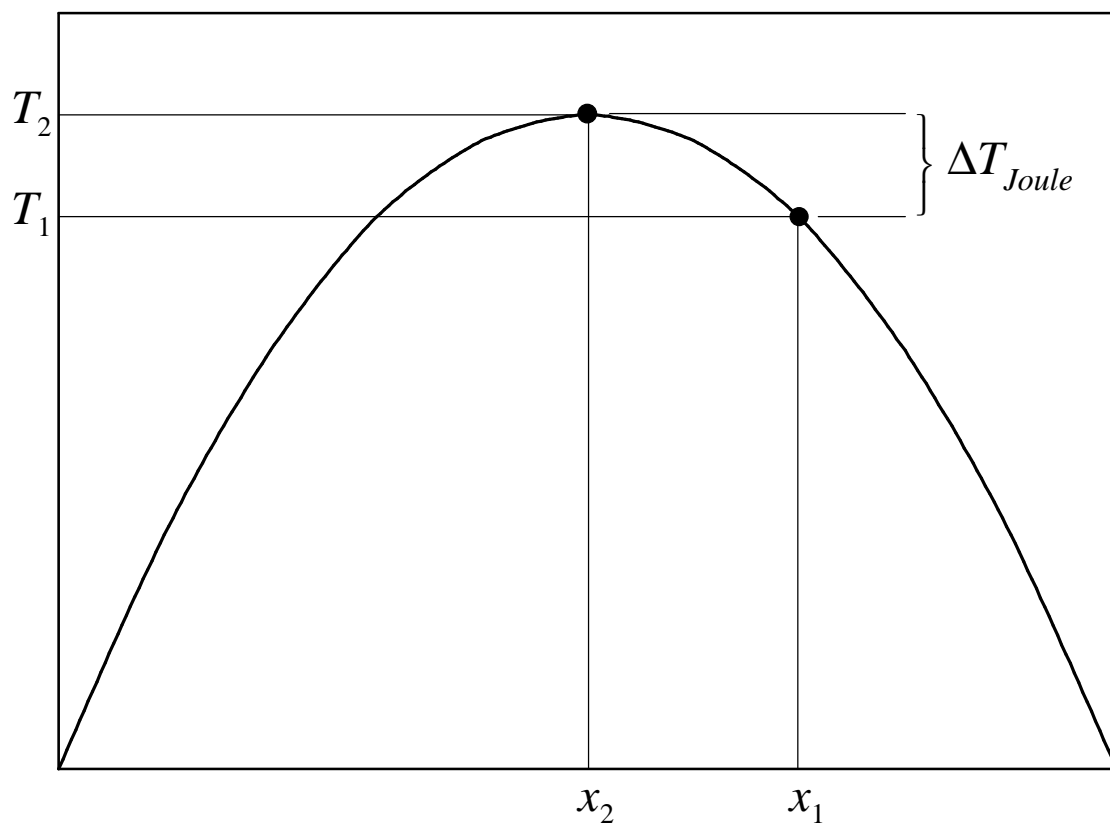
REFERENCES

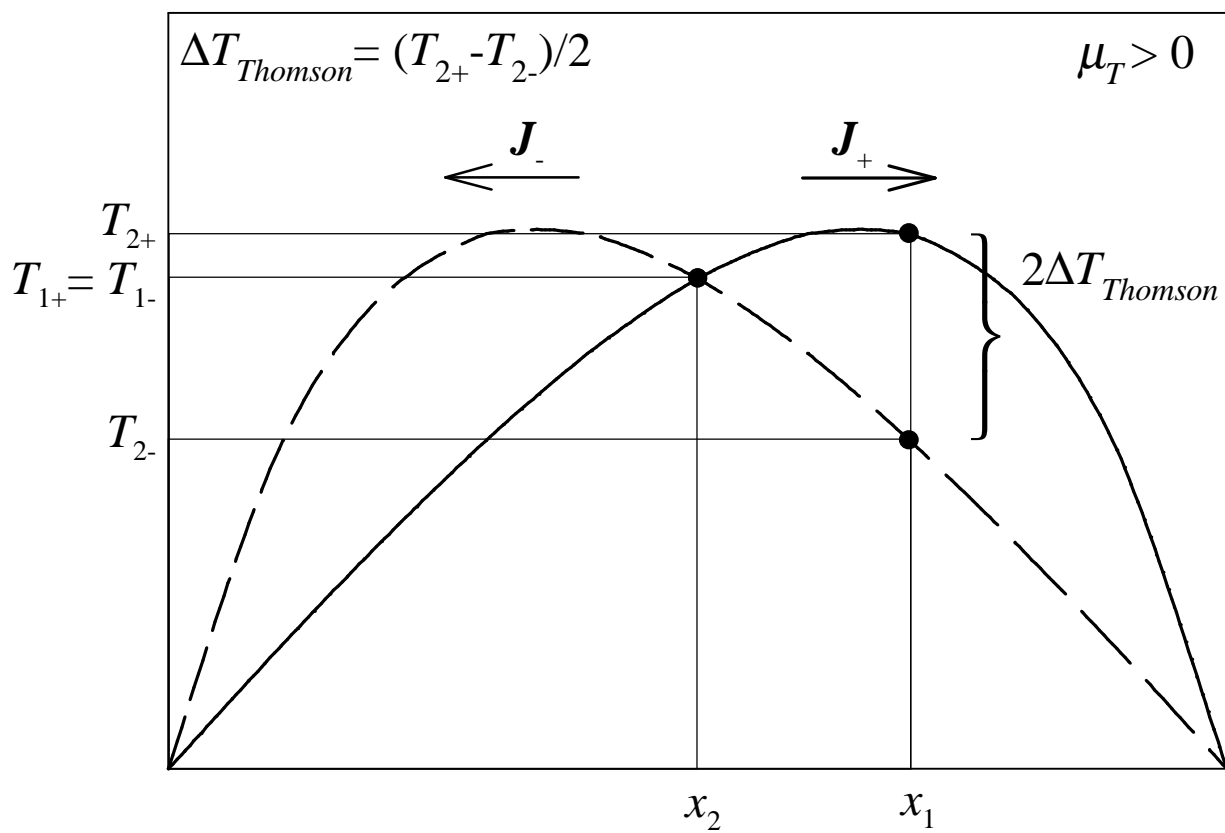
- [1] S.D.Obertelli, J.R.Cooper and J.L.Tallon, Phys.Rev.B **46** 14928 (1992).
- [2] see e.g. S.Martin, A.T.Fiory, R.M.Fleming, L.F.Schneemeyer and J.V.Waszcak, Phys.Rev.B **41** 846 (1990).
- [3] Y.Kubo and T.Manako, Physica C **197** 178 (1992).
- [4] P.W.Bridgman, Phys.Rev. **24**, 644 (1924).
- [5] B.V.Paranjape and J.S.Levinger, Phys.Rev. **120**, 437 (1960).
- [6] H.Fieber, A.Nedoluha and K.M.Koch, Z.Physik **131**, 143 (1952).
- [7] H.Mette, W.W.Gärtner and C.Loscoe, Phys.Rev. **115**, 537 (1959) .
- [8] H.Mette, W.W.Gärtner and C.Loscoe, Phys.Rev. **117**, 1491 (1960) .
- [9] E.H.Putley, The Proceedings of the Physical Society, Sect. B, part 1, **68**, 35 (1955).
- [10] *International Critical Tables* (Mc-Graw-Hill Book Company, Inc., New York, 1929), vol. 6, p.419
- [11] L.Zecchina, phys.stat.sol. **42**, K153 (1970).
- [12] J.A.Clayhold, A.W.Linnen, Jr., F.Chen and C.W.Chu, Phys.Rev.B **50**, 4252 (1994).
- [13] V.E.Gasumyants, N.V.Ageev, I.E.Goldberg and V.I.Kaydanov, Physica C **282-287**, 1279 (1997).
- [14] P.Fournier, X.Jiang, W.Jiang, S.N.Mao, T.Venkatesan, C.J.Lobb and R.L.Greene, Phys.Rev.B **56**, 14149 (1997).
- [15] F.Devaux, A.Manthiram and J.B.Goodenough, Phys.Rev.B **41**, 8723 (1990).
- [16] M.Suzuki, Phys.Rev.B **39**, 2312 (1989).
- [17] H.Takagi, T.Ido, S.Ishibashi, M.Uota, S.Uchida and Y.Tokura, Phys.Rev.B **40**, 2254 (1989).
- [18] J.R.Cooper, B.Alavi, L.W.Zhou, W.P.Beyerman, G.Grüner, Phys.Rev.B **35**, 8794 (1987).
- [19] J.B.Goodenough and A.Manthiram, in *Studies of High Temperature Superconductors*, vol.5, Ed. by A.V.Narlikar, Plenum Press, New York, 1990.

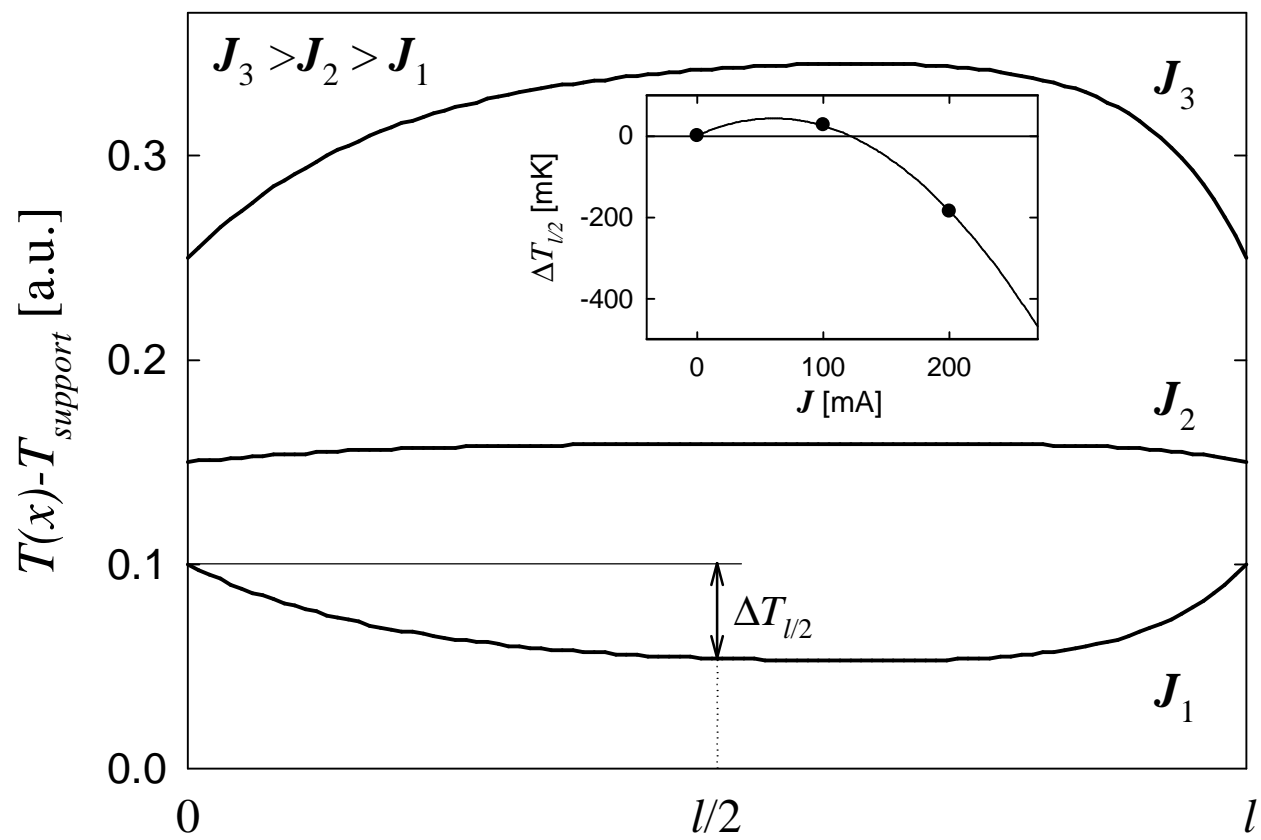




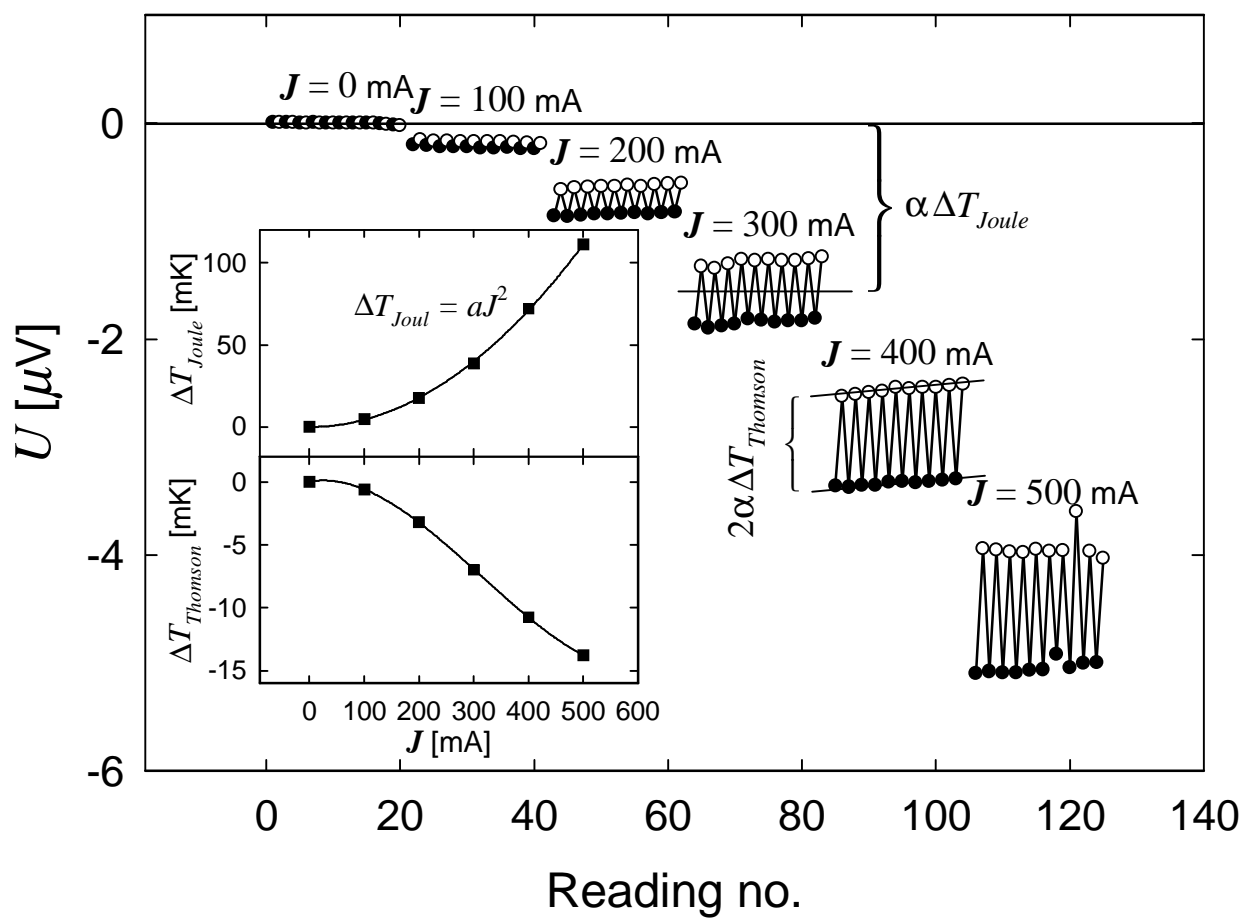




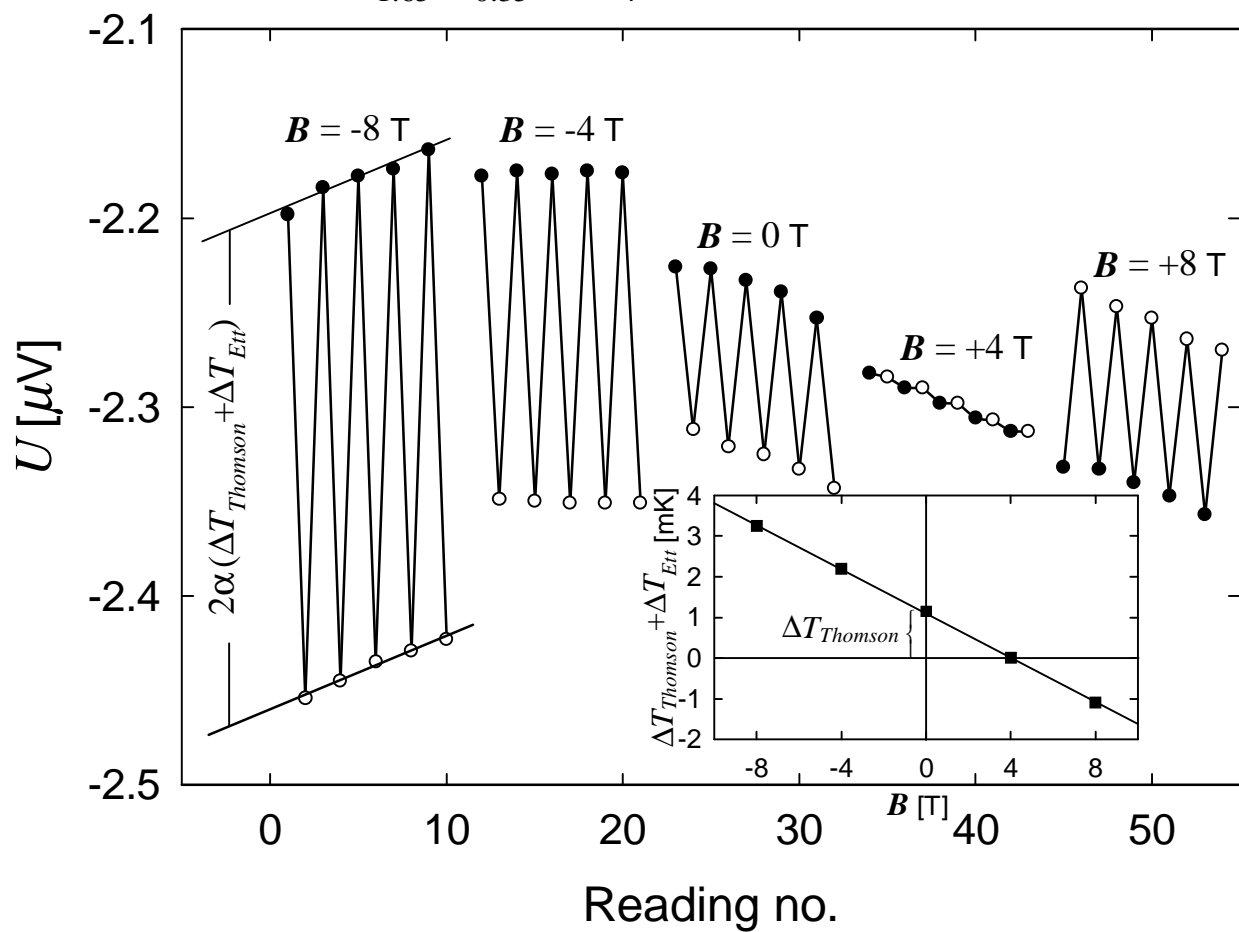




$\text{La}_{1.75}\text{Sr}_{0.25}\text{CuO}_4$, $B = 0$ T, $T = 300$ K



$\text{La}_{1.65}\text{Sr}_{0.35}\text{CuO}_4$, $J = 400 \text{ mA}$, $T = 300 \text{ K}$



La_{1.85}Sr_{0.15}CuO₄, $T = 300$ K

